Inorganic Chemistry
Article

Inorg. Chem. **2011**, *50*, 1361–1367 **1361**
DOI: 10.1021/ic101997b

Nature of Intramolecular Transannular Interaction in Group 13 Atranes: A Theoretical Study

Ashwini K. Phukan* and Ankur Kanti Guha

Department of Chemical Sciences, Tezpur University, Napaam 784028, Assam, India

Received September 30, 2010

Ab initio molecular orbital (MO) calculations at the MP2/6-31+G* level coupled with quantum theory of atoms in molecules (QTAIM) analysis were carried out on group 13 atranes (M = B, Al, Ga) with special emphasis on the nature of the transannular M···N interaction present in these molecules. Substituents at the equatorial position were found to influence the extent of transannular interaction. Boratrane molecules were found to have the strongest M···N interaction and consequently have higher stabilization energies. QTAIM analysis revealed the presence of significant covalent character in the transannular M···N bonds which decreases down the group.

1. Introduction

The need to prepare nitride ceramic materials and semiconductors has prompted researchers to look for new synthetic targets featuring group 13 elements bonded to nitrogen.[1] Among them, the use of symmetrical tripodal ligands such as polydentate chelating tetramine and its derivatives to form atranes have attracted interest as early as 1951.[2] These tetramine ligands bind to the metal center in a tetradentate manner to create a sterically protected, 3-fold-symmetric pocket around the metal center.[3a] Since their first isolation in 1951, numerous group 13 atranes have been reported in the literature (Table 1).[3−5,8] These atranes (Scheme 1) are characterized by high thermodynamic stability and resistance to hydrolysis which is believed to be due to the presence of an intramolecular transannular M···N bond in them.

This interaction accounts for various properties of these atranes. The strength of this transannular M···N interaction is found to depend on the nature of substituents at the equatorial (E) positions.[3a] For example, the transannular B···N bond is stronger in carbaboratranes (M = B, E = CH_2) than in oxaboratranes (M = B, E = O), as revealed by photoelectron spectroscopy.[3a]

The atrane molecules formed by the first three members of group 13 are found to exist in various structural forms. For example, alumatrane (M = Al, E = O, NR) exists as a dimer in gas phase, as a monomer, hexamer, and octamer in solution, and as a tetramer in solid state.[3,4] In 2003, Verkade and co-workers reported the first structurally characterized monomeric oxaalumatrane (M = Al, E = O) in all the three phases.[3g] Carbagallatranes (M = Ga, E = CH_2) were reported to be a very stable solid.[4a] Verkade and co-workers[3e] synthesized monomeric azagallatranes (M = Ga, E = NR) and confirmed the structure with the help of NMR techniques.

*To whom correspondence should be addressed. Phone: +91 (3712) 267173. Fax: +91 (3712) 267005. E-mail: ashwini@tezu.ernet.in.

(1) (a) Verkade, J. G. *Acc. Chem. Res.* **1993**, *26*, 483–489. (b) Paine, R. T.; Narula, C. K. *Chem. Rev.* **1990**, *90*, 73–91. (c) Wade, T.; Park, J.; Garza, E. G.; Ross, C. B.; Smith, D. M.; Crooks, R. M. *J. Am. Chem. Soc.* **1992**, *114*, 9457–9464. (d) Cowley, A. H.; Jones, R. A. *Angew. Chem., Int. Ed. Engl.* **1989**, *28*, 1208–1215. (e) Riedel, R.; Schaible, S.; Klingebiel, V.; Noltemeyer, M.; Werner, E. *Z. Anorg. Allg. Chem.* **1991**, *603*, 119.

(2) Brown, H. C.; Fletcher, E. A. *J. Am. Chem. Soc.* **1951**, *73*, 2808–2813.

(3) (a) Verkade, J. G. *Coord. Chem. Rev.* **1994**, *137*, 233–295. (b) Müller, E.; Bürgi, H. B. *Helv. Chim. Acta* **1984**, *67*, 399–405. (c) Mattes, R.; Fenske, D.; Tebbe, K.−F. *Chem. Ber.* **1972**, *105*, 2089–2094. (d) Pinkas, J.; Wang, T.; Jacobson, R. A.; Verkade, J. G. *Inorg. Chem.* **1994**, *33*, 4202–4210. (e) Pinkas, J.; Wang, T.; Jacobson, R. A.; Verkade, J. G. *Inorg. Chem.* **1994**, *33*, 5244–5253. (f) Kurlyukov, A. A.; Lyssenko, K. A.; Antipin, M. Y.; Kirin, V. N.; Chernyshev, E. A.; Knyazev, S. P. *Inorg. Chem.* **2002**, *41*, 5043–5051. (g) Kim, Y.; Verkade, J. G. *Inorg. Chem.* **2003**, *42*, 4804–4806. (h) Hein, F.; Albert, P. W. *Z. Anorg. Allg. Chem.* **1952**, *269*, 67. (i) Mehrotra, R. C.; Mehrotra, R. K. *J. Indian Chem. Soc.* **1962**, *39*, 677. (j) Healy, M. D.; Barron, A. R. *J. Am. Chem. Soc.* **1989**, *111*, 398–399. (k) Karlov, S. S.; Selina, A. A.; Chernyshova, E. S.; Oprunenko, Y. F.; Merkulov, A. A.; Tafeenko, V. A.; Churakov, A. V.; Howard, J. A. K.; Zeitseva, G. S. *Inorg. Chim. Acta* **2007**, *360*, 563–578.

(4) (a) Schumann, H.; Hartmann, U.; Dietrich, A.; Pickhardt, J. *Angew. Chem., Int. Ed. Engl.* **1988**, *27*, 1077–1078. (b) Schumann, H.; Hartmann, U.; Wassermann, W.; Just, O.; Dietrich, A.; Pohl, L.; Hostauk, M.; Lokai, M. *Chem. Ber.* **1991**, *124*, 1113–1119. (c) Pinkas, J.; Verkade, J. G. *Phosphorus, Sulfur Silicon Relat. Elem.* **1994**, *93*, 333–337. (d) Shutov, P. L.; Karlov, S. S.; Harms, K.; Churakov, A. V.; Lorberth, J.; Zaitseva, G. S. *Eur. J. Inorg. Chem.* **2004**, 2123–2129.

(5) (a) Lee, K. J.; Livant, P. D.; McKee, M. L. M.; Worley, S. D. *J. Am. Chem. Soc.* **1985**, *107*, 5901–5906. (b) Li, E.; Xu, G.; Wang, T.; Lu, K.; Wu, G.; Tao, J.; Feng, Y. *Huaxue Tongbao* **1985**, *6*, 22; *Chem. Abstr.* **1986**, *104*, 121849h. (c) Wang, T.; Lu, K.; Wu, G. *Huaxue Tongbao* **1986**, *5*, 33; *Chem. Abstr.* **1987**, *105*, 202098k.

(6) (a) Schimdt, M. W.; Windus, T. L.; Gordon, M. S. *J. Am. Chem. Soc.* **1995**, *117*, 7480–7486. (b) Trofimov, A. B.; Zakrzewski, V. G.; Dolgounitcheva, O.; Ortiz, J. V.; Sidorkin, V. F.; Belogolova, E. F.; Pestunovich, V. A. *J. Am. Chem. Soc.* **2005**, *127*, 986–995. (c) Karlov, S. S.; Tyurin, D. A.; Zabalov, M. V.; Churakov, A. V.; Zaitseva, G. S. *Theochem* **2005**, *724*, 31–37. (d) Sidorkin, V. F.; Belogolova, E. F.; Gordon, M. S.; Lazarevich, M. I.; Lazareva, N. F. *Organometallics* **2007**, *26*, 4568–4574.

Published on Web 01/19/2011

Table 1. List of Experimentally Known Monomeric Group 13 Atranes for Which X-ray Crystal Structures Are Available

group 13 elements (M)	equatorial group (E)	ranges of r(M···N) in Å	ref
B	O	1.622−1.684	3b, 3k
Al	O	1.921−2.083	3g, 8
	$NSiMe_3$	1.983	3d
Ga	CH_2	2.094	4a

Scheme 1

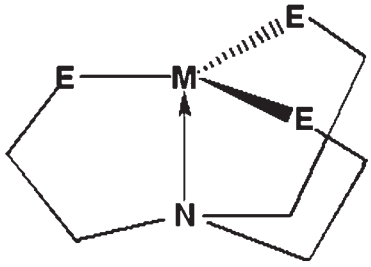

M = B, Al, Ga;

E = CH_2, SiH_2, NH, NMe, $NSiH_3$, PH, PMe, $PSiH_3$, O, S, Se

However, to the best of our knowledge, no X-ray data is available for monomeric azagallatranes, although that of dimeric azagallatranes are known.[3e]

There are extensive theoretical and experimental reports in the literature about atranes of group 14 and 15 elements, especially those of silatranes[6,3f] and phosphatranes.[7] However, theoretical studies on group 13 atranes are very limited,[3f,8] even though there exists a large body of experimental literature on these molecules.[3−5,8] Korlyukov and co-workers have carried out a combined experimental and theoretical study on the intramolecular transannular interaction and cage effect of boratrane (M = B, E = NH, CH_2, O, S) and 1-methylsilatrane.[3f] They found a stronger transannular bond in boratrane than 1-methylsilatrane and verified it theoretically with the help of Bader's atoms in molecules (AIM)[9] theory. They concluded that the transannular B···N bond had a characteristic of a "shared" (covalent) type of interaction. An experimental and theoretical study made by Su and co-workers demonstrated the importance of introducing steric protection near the vacant fifth coordination site of aluminum in realizing the monomeric form of oxaalumatrane.[8] On the basis of theoretical investigation, they concluded that the acidity of pro-oxaalumatrane (a pro-atrane is a molecule with no transannular M···N bond[1a]) was higher than boron trifluoride. Thus, to the best of our knowledge, so far, there is no systematic theoretical study on the structure and reactivity of group 13 atranes. Hence, it is worthwhile to carry out a systematic theoretical study on group 13 atranes as the organometallic derivatives of these atranes are important reagents in various transformations.[10] We present here a comprehensive theoretical study on the structure and stability of neutral group 13 atranes (M = B, Al, Ga; Scheme 1). The number of equatorial substituents considered in this study is considerably larger than the experimentally available geometries so as to extend the list of probable atrane molecules formed by these group 13 elements. The main emphasis of our study will be the nature of the intramolecular transannular M···N interaction of group 13 atranes as many of their properties are dictated by this interaction. In all our discussions, we will use the prefix carba, sila, aza, azamethyl, azasilyl, phospha, phosphamethyl, phosphasilyl, oxa, thia, and selena to indicate the atranes with CH_2, SiH_2, NH, NMe, $NSiH_3$, PH, PMe, $PSiH_3$, O, S, and Se, respectively, as the equatorial substituents.

2. Computational Details

All the structures were fully optimized at the gradient-corrected density functional theory (DFT) using the Becke's three-parameter hybrid functional (B3LYP) with correlation functional of Lee, Yang, and Parr.[11] The 6-31+G* basis set was employed for all the elements.[12] Frequency calculations were performed at the same level of theory to verify the nature of the stationary state. All structures were identified as the ground state as their respective Hessian (matrix of analytically determined second derivative of energy) was real. Since the geometrical parameters obtained at the B3LYP/6-31+G* level of theory are not in good agreement with experimental results, we have further optimized these molecules at MP2 level (Møller−Plesset perturbation theory terminated at second order) of ab initio molecular orbital (MO) theory using the same basis set.[13] Bonding nature of all the compounds were analyzed using natural bonding analysis (NBO).[14a,b] The strength of individual bonds has been ascertained from their values of Wiberg bond indices (WBI)[14c] available within the NBO routine. All the calculations were performed using the Gaussian 03 suite of program.[15] All our discussions are based only on results obtained at the MP2/6-31+G* level of theory. In the discussion, pyramidalization angle around a particular atom X (denoted by θ_X) refers to the difference of the sum of the angles around X from the ideal value of 360°, i.e., θ_X (in degrees) = $360 - \sum\theta_X$, where X = M (B, Al, Ga), N (bridgehead nitrogen atom), and E (equatorial atom).

In order to get an in-depth understanding of the bonding in these compounds, topological analysis of the electron density $\rho(r)$ was performed with Bader's quantum theory of atoms in molecules (QTAIM).[9] This is done by first generating the wave function file from the optimized structures using Gaussian 03 and then analyzing with the program AIMALL.[16]

(7) (a) Windus, T. L.; Schimdt, M. W.; Gordon, M. S. *J. Am. Chem. Soc.* **1994**, *116*, 11449–11455. (b) Galasso, V. *J. Phys. Chem. A* **2004**, *108*, 4497–4504. (c) Kárpáti, T.; Veszprémi, T.; Thirupathi, N.; Liu, X.; Wang, Z; Ellern, A.; Nyulászi, L.; Verkade, J. G. *J. Am. Chem. Soc.* **2006**, *128*, 1500–1512. (d) Kobayashi, J.; Goto, K.; Kawashima, T.; Schimdt, M. W.; Nagase, S. *J. Am. Chem. Soc.* **2002**, *124*, 3703–3712.

(8) Su, W.; Kobayashi, J.; Ellern, A.; Kawashima, T.; Verkade, J. G. *Inorg. Chem.* **2007**, *46*, 7953–7959.

(9) Bader, R. W. F. *Atoms in Molecules: a Quantum Theory*; Oxford University Press: Oxford, U. K., 1990.

(10) (a) Nelson, S. G.; Kim, B.−K.; Peelen, T. *J. Am. Chem. Soc.* **2000**, *122*, 9318–9319. (b) Ooi, T.; Uraguchi, D.; Kogashima, N.; Maruoka, K. *J. Am. Chem. Soc.* **1998**, *120*, 5327–5328.

(11) B3LYP is Becke's three-parameter hybrid method using the LYP correlation functional. (a) Becke, A. D. *J. Chem. Phys.* **1993**, *98*, 5648–5652. (b) Lee, C.; Yang, W.; Parr, R. G. *Phys. Rev. B* **1988**, *37*, 785–789. (c) Vosko, S. H.; Wilk, L.; Nusair, M. *Can. J. Phys.* **1980**, *58*, 1200–1211.

(12) (a) Hehre, W. J.; Ditchfield, R.; Pople, J. A. *J. Chem. Phys.* **1972**, *56*, 2257–2261. (b) Hariharan, P. C.; Pople, J. A. *Theo. Chim. Acta* **1973**, *28*, 213–222. (c) Gordon, M. S. *Chem. Phys. Lett.* **1980**, *76*, 163–168.

(13) (a) Møller, C.; Plesset, M. S. *Phys. Rev.* **1934**, *46*, 618–622. (b) Binkley, J. S.; Pople, J. A. *Int. J. Quantum Chem.* **1975**, *9S*, 229–236.

(14) (a) Glendening, E. D.; Reed, A. E.; Carpenter, J. E.; Weinhold, F. *NBO Program 3.1*; University of Wisconsin: Madison, WI, 1988. (b) Reed, A. E.; Weinhold, F.; Curtiss, L. A. *Chem. Rev.* **1988**, *88*, 899–926. (c) Wiberg, K. B. *Tetrahedron* **1968**, *24*, 1083–1096.

(15) Frisch, M. C. et al. *Gaussian 03*, revision D.02; Gaussian, Inc.: Wallingford, CT, 2004. For complete reference, see Supporting Information.

(16) Keith, T. A. *AIMAll* (Version 10.05.04, Professional); **2010** (http://aim.tkgristmill.com).

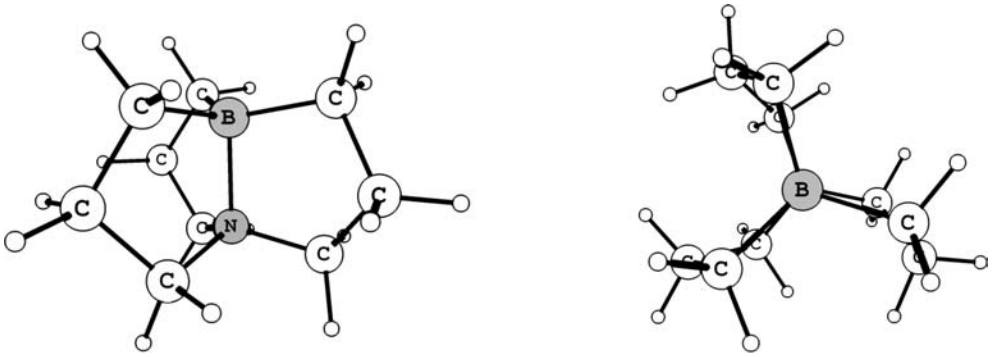

Figure 1. Optimized geometry of a group 13 atrane (M = B, E = CH_2) molecule shown in two different perspectives.

Table 2. MP2/6-31+G* Computed Transannular ($r_{M\cdots N}$) Distances in Å, Pyramidalizaion Angles Around Group 13 Elements (θ_M), Bridgehead Nitrogen Atom (θ_N) and Equatorial Substituents (θ_E) in Degrees, M−E Distances ($r_{M\text{-}E}$) in Å and Natural Charges at M (q_M), Bridgehead Nitrogen (q_N), and Equatorial Substituents (q_E)[a]

		Group 13 Elements		
equatorial substituents (E)	geometric parameters	B	Al	Ga
CH_2	$r_{M\cdots N}$	1.716 (0.459)	2.063 (0.171)	2.123 (0.188)
	θ_M/θ_N	8.7/22.1	0.02/21.3	0.2/19.9
	$r_{M\text{-}E}$	1.629 (0.853)	2.005 (0.512)	2.021 (0.580)
	$q_M/q_N/q_E$	0.790/−0.617/−0.756	1.869/−0.743/−1.063	1.655/−0.714/−1.0
SiH_2	$r_{M\cdots N}$	1.655 (0.594)	2.134 (0.213)	2.175 (0.230)
	θ_M/θ_N	8.8/33.1	0.50/33.3	0.5/33.3
	$r_{M\text{-}E}$	2.007 (0.921)	2.445 (0.899)	2.404 (0.913)
	$q_M/q_N/q_E$	−1.063/−0.578/1.159	0.603/−0.728/0.623	0.417/−0.696/0.682
NH	$r_{M\cdots N}$	1.769 (0.387)	2.000 (0.176)	2.093 (0.189)
	$\theta_M/\theta_N/\theta_E$	8.5/16.4/23.5	0.05/18.5/12.1	0.8/19.0/21.4
	$r_{M\text{-}E}$	1.518 (0.753)	1.851 (0.437)	1.958 (0.491)
	$q_M/q_N/q_E$	1.239/−0.638/−1.029	2.089/−0.747/−1.269	1.924/−0.725/−1.219
NMe	$r_{M\cdots N}$	1.693 (0.435)	1.983 (0.162)	2.092 (0.175)
	$\theta_M/\theta_N/\theta_E$	10.6/17.6/22.0	0.02/17.6/9.7	0.6/19.0/17.9
	$r_{M\text{-}E}$	1.523 (0.693)	1.857 (0.393)	1.982 (0.457)
	$q_M/q_N/q_E$	1.312/−0.639/−0.904	2.125/−0.758/−1.084	1.937/−0.730/−1.022
$NSiH_3$	$r_{M\cdots N}$	1.652 (0.425)	2.000 (0.155)	2.038 (0.176)
	$\theta_M/\theta_N/\theta_E$	10.1/14.5/11.6	0.04/17.5/1.6	0.2/18.5/1.6
	$r_{M\text{-}E}$	1.512 (0.706)	1.847 (0.358)	1.930 (0.420)
	$q_M/q_N/q_E$	1.288/−0.634/−1.302	2.186/−0.759/−1.521	2.035/−0.733/−1.478
PH	$r_{M\cdots N}$	1.671 (0.535)	2.052 (0.185)	2.108 (0.204)
	$\theta_M/\theta_N/\theta_E$	18.2/29.8/75.9	0.30/27.3/74.6	0.1/25.1/76.2
	$r_{M\text{-}E}$	1.974 (1.009)	2.364 (0.772)	2.358 (0.798)
	$q_M/q_N/q_E$	−0.392/−0.623/0.423	1.145/−0.756/−0.092	0.940/−0.721/−0.029
PMe	$r_{M\cdots N}$	1.666 (0.536)	2.064 (0.182)	2.119 (0.201)
	$\theta_M/\theta_N/\theta_E$	18.4/29.8/63.9	0.1/28.2/65.1	0.05/26.0/67.7
	$r_{M\text{-}E}$	1.985 (1.000)	2.366 (0.749)	2.362 (0.781)
	$q_M/q_N/q_E$	−0.405/−0.624/0.648	1.174/−0.758/0.143	0.928/−0.721/0.215
$PSiH_3$	$r_{M\cdots N}$	1.651 (0.543)	2.053 (0.181)	2.113 (0.203)
	$\theta_M/\theta_N/\theta_E$	17.1/30.0/60.5	0.06/28.0/65.9	0.01/25.8/68.6
	$r_{M\text{-}E}$	1.992 (0.997)	2.351 (0.743)	2.353 (0.776)
	$q_M/q_N/q_E$	−0.289/−0.636/0.142	1.227/−0.763/−0.356	0.998/−0.725/−0.288
O	$r_{M\cdots N}$	1.735 (0.382)	2.013 (0.163)	2.018 (0.193)
	θ_M/θ_N	10.8/13.3	0.3/14.3	0.30/13.8
	$r_{M\text{-}E}$	1.443 (0.673)	1.766 (0.377)	1.834 (0.411)
	$q_M/q_N/q_E$	1.473/−0.653/−0.863	2.228/−0.756/−1.046	2.109/−0.740/−1.000
S	$r_{M\cdots N}$	1.672 (0.509)	2.040 (0.190)	2.104 (0.206)
	θ_M/θ_N	15.2/26.4	1.8/25.1	0.9/23.0
	$r_{M\text{-}E}$	1.896 (1.011)	2.224 (0.728)	2.243 (0.758)
	$q_M/q_N/q_E$	0.099/−0.647/0.009	1.402/−0.761/−0.383	1.226/−0.724/−0.339
Se	$r_{M\cdots N}$	1.649 (0.527)	2.029 (0.185)	2.089 (0.208)
	θ_M/θ_N	16.7/29.6	1.3/26.7	0.9/25.0
	$r_{M\text{-}E}$	2.022 (1.025)	2.345 (0.789)	2.356 (0.811)
	$q_M/q_N/q_E$	−0.111/−0.653/0.120	1.211/−0.760/−0.287	1.032/−0.722/−0.235

[a] The respective Wiberg bond index (WBI) values are given within parentheses.

3. Results and Discussion

3.1. Molecular Geometry. All these group 13 atranes possess a pseudotetrahedral geometry around the central group 13 element having a transannular M···N bond (Figure 1). The optimized geometries of these molecules possess a local C_3 axis of symmetry, and the atrane

framework consists of three five-member envelope shaped rings with both the group 13 element and bridgehead nitrogen atoms inwardly pyramidalized. The gas phase geometries show elongation of the transannular M···N bonds compared to solid phase. This feature is a characteristic of "partially bonded molecules" as referred to in the literature.[17]

As stated above, the gas phase geometries of boratranes show elongation of the transannular B···N bonds compared to solid phase (up to 0.06 Å for oxaboratranes; Table 2).[3f] The calculated transannular B···N distances are found to be very close to the sum of the covalent radii of B and N (1.65 Å) (Table 2). The geometrical variation, i.e., the changes in pyramidalization angle around M (θ_M) and bridgehead nitrogen atom (θ_N), is an indication of the strength of this transannular interaction. In general, a higher value of pyramidalization around both M (θ_M) and N (θ_N) results in a closer approach of both the transannular atoms (B and N) which in turn enhances the transannular interaction. While θ_M does not vary significantly, θ_N changes appreciably with changes in the nature of equatorial atoms (Figure 2). The highest value of θ_M and θ_N is computed for sila, phosphasilyl, and selena boratranes, and accordingly, shorter B···N distances are computed for these molecules. However, in spite of a smaller value of θ_N, the B···N bond of azasilylboratrane is quite short. The shortening of transannular distance for azasilyl boratrane may be due to the bulky SiH_3 group which occupies a larger volume of space than either hydrogen or methyl, resulting in steric crowding around the central boron atom. In order to reduce this steric crowding, the boron atom moves toward the bridgehead nitrogen atom resulting in enhanced B···N interaction. Among all the boratranes considered, the longest transannular B···N bond is found for azaboratrane. This is also reflected in the values of θ_M and θ_N which are found to be the lowest for this molecule. Transannular B···N bonds are found to be stronger with phosphaboratrane derivatives compared to azaboratrane derivatives. This may be due to a higher degree of pyramidalization at the equatorial phosphorus atoms compared to nitrogen which is expected due to higher inversion barrier at phosphorus than nitrogen. The high pyramidalization at equatorial phosphorus atoms results in less π delocalization from the phosphorus to boron atom rendering the boron atom electron deficient. Hence, it can readily accept electron density from the bridgehead nitrogen atom. Donation of a lone pair of electron density from the equatorial oxygen atom to the formally empty boron p_π orbital results in weakening of the transannular interaction. Thus, the π-donating ability of the equatorial groups as well as the steric bulk at the equatorial position play a decisive role in deciding the extent of transannular interaction. The M−E bond strengths are consistent with the electronegativity difference between the participating atoms. The highest M−E bond strength (as revealed by WBI values of respective bonds, Table 2) is computed for selenaboratranes while the lowest is computed for oxaboratranes. Higher M−E bond strengths are computed for phosphaboratrane derivatives than their aza analogs. This is also due to the lower polarity of the B−P bond compared to B−N bond.

The computed geometrical parameters of alumatranes and gallatranes are in excellent agreement with the experimental structures.[3d,4a] The transannular Al···N and Ga···N distances are very close to the sum of the covalent radii of Al and N (2.05 Å) and Ga and N (1.95 Å), respectively (Table 2). However, transannular Al···N and Ga···N bonds are weaker than B···N bonds as revealed by the smaller Wiberg bond index (WBI) values (Table 2). This is due to the fact that the heavier aluminum

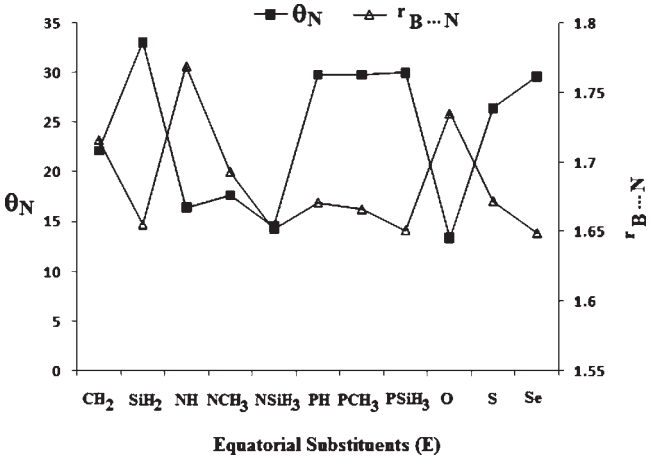

Figure 2. Variation of transannular B···N distances [$r_{B\ldots N}$ in Å] with pyramidalization angle at the bridgehead nitrogen atom (θ_N in degrees).

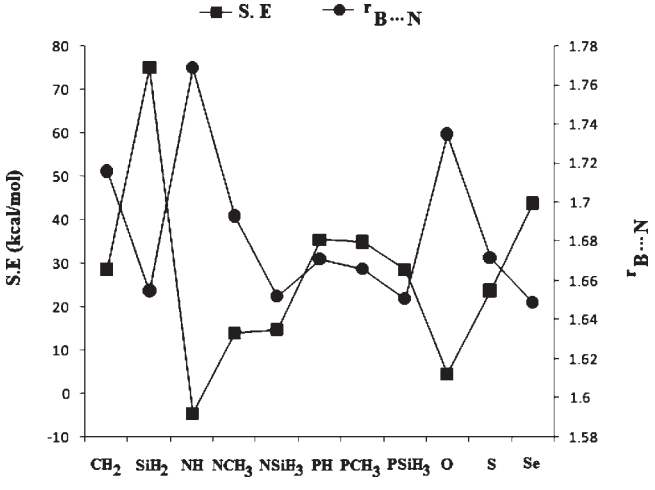

Figure 3. Variation of stabilization energies (SE in kcal/mol) with transannular B···N distances ($r_{B\ldots N}$ in Å).

Table 3. Stabilization Energies (kcal/mol) of Group 13 Atranes for Different Equatorial Substituents Computed at the MP2/6-31+G* Level of Theory

	substituents at the equatorial position (E)										
group 13 elements (M)	CH_2	SiH_2	NH	NMe	$NSiH_3$	PH	PMe	$PSiH_3$	O	S	Se
B	28.6	75.0	−4.6	14.0	14.7	35.4	34.9	28.5	4.5	23.8	43.8
Al	25.4	54.2	11.6	26.5	25.4	27.4	32.6	29.6	20.2	32.4	43.7
Ga	30.3	57.5	22.9	32.3	33.6	27.5	34.9	30.5	42.6	32.7	46.1

Table 4. Electron Density ρ, Laplacian of Electron Density $\nabla^2\rho$, and Local Energy Density $H(r)$ at the M···N Bond Critical Point of Group 13 Atranes[a]

		substituents at the equatorial position (E)										
group 13 elements (M)	AIM parameters	CH_2	SiH_2	NH	NCH_3	$NSiH_3$	PH	PCH_3	$PSiH_3$	O	S	Se
B	ρ	0.100	0.113	0.096	0.110	0.121	0.113	0.114	0.119	0.106	0.118	0.124
	$\nabla^2\rho$	0.315	0.411	0.137	0.250	0.302	0.320	0.333	0.326	0.136	0.245	0.276
	$H(r)$	−0.068	−0.077	−0.075	−0.083	−0.092	−0.081	−0.081	−0.087	−0.085	−0.091	−0.095
Al	ρ	0.051	0.045	0.058	0.061	0.059	0.054	0.052	0.054	0.058	0.055	0.057
	$\nabla^2\rho$	0.275	0.211	0.341	0.367	0.342	0.280	0.268	0.277	0.329	0.29	0.30
	$H(r)$	−0.001	−0.003	−0.001	−0.001	−0.001	−0.002	−0.003	−0.003	−0.002	−0.003	−0.003
Ga	ρ	0.066	0.060	0.069	0.068	0.072	0.069	0.068	0.069	0.086	0.071	0.073
	$\nabla^2\rho$	0.251	0.200	0.285	0.289	0.296	0.255	0.246	0.249	0.354	0.256	0.270
	$H(r)$	−0.016	−0.015	−0.016	−0.016	−0.017	−0.018	−0.018	−0.019	−0.024	−0.019	−0.02

[a] All values are in a.u.

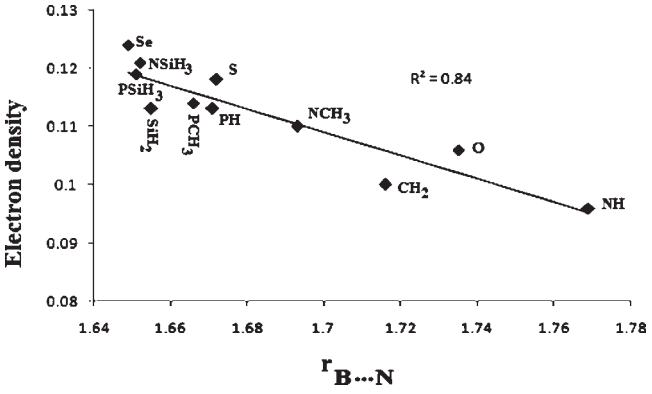

Figure 4. Variation of transannular B···N distances (Å) of all the boratrane molecules under consideration with electron density ρ_b (a.u.).

and gallium atoms in the atrane cage attain nearly a planar arrangement as revealed by very low values of θ_M. Although the bridgehead nitrogen atom has similar pyramidalization as computed for boratranes, low pyramidalization around aluminum and gallium atoms lead to the weakening of the transannular bond. The transannular M···N distances in heavier group 13 atranes show a different trend than those observed for boratranes. For example, in contrast to boratranes, the observed variation in transannular Al···N and Ga···N distances do not correlate with θ_M and θ_N. Longer transannular distances are computed for sila substituted alumatranes and gallatranes. This might be due to the involvement of bigger aluminum or gallium atoms and equatorial silicon atoms in the atrane framework which restricts the metal atom (Al or Ga) to come in close proximity with the bridgehead nitrogen atom for an effective transannular interaction. However, no such steric hindrance is there for the lighter boron atom. In order to investigate the cage effect induced by the atrane framework on the transannular M···N distance, we have also optimized some donor−acceptor complexes of the type $NH_3 \rightarrow M(EH)_3$ (Scheme S1) at the same level of theory (MP2/6-31+G*).

It is interesting to note that the transannular B···N distances in the cyclic atranes are slightly longer (≈0.03 Å) than those in the respective donor−acceptor complexes (Table S1, Supporting Information). Hence, the atrane cage has no significant effect on the transannular B···N distances of boratranes. However, transannular M···N distances in alumatranes and gallatranes are found to be slightly shorter than those of the respective acyclic donor−acceptor complexes. Thus, the cyclic atrane framework induces a cage effect in heavier group 13 atranes, resulting in strengthening of the transannular M···N bonds compared to the respective acyclic donor−acceptor complexes.

3.2. Stabilization Energy. The stability of these group 13 atranes is largely governed by the degree of M···N interaction with significant contribution coming from strengthening of M−E bonds. We have used three sets of equations (eqs 1−3) to compute their stabilization energies (Table 3).

$$M(EH_2CH_2CH_2)_3N + 6CH_4 \rightarrow (CH_3CH_2)_3N + M(EH_3)_3 + 3C_2H_6$$
$$M = B, Al, Ga; E = C, Si \quad (1)$$

$$M(ERCH_2CH_2)_3N + 3EH_3 + 3CH_4 \rightarrow (CH_3CH_2)_3N + M(EHR_3)_3 + 3CH_3EH_2$$
$$M = B, Al, Ga; E = N, P; R = H, CH_3, SiH_3 \quad (2)$$

$$M(ECH_2CH_2)_3N + 3H_2E + 3CH_4 \rightarrow (CH_3CH_2)_3N + M(EH)_3 + 3CH_3EH$$
$$M = B, Al, Ga; E = O, S, Se \quad (3)$$

With few exceptions, stabilization energies of boratranes are found to be higher for those with stronger transannular B···N bonds (Figure 3). The highest and lowest values of stabilization energies are computed for sila and azaboratranes, respectively, as the B···N bond of the former is shorter than the latter (Table 2). However, phosphaboratrane derivatives show a different trend, i.e., their stabilization energies decrease with an increase in transannular interaction which is caused by shortening of the M−E bonds. Unlike boratranes, we could not find any correlation between the M···N bond strength and stabilization energy for heavier group 13 atranes. It is interesting to note that replacement of the equatorial CH_2 group by SiH_2 dramatically increases the stability of all the group 13 atranes. For the chalcogen substituted atranes, the stability order is O < S < Se for boratranes and alumatranes while, for gallatranes, the order is S < O < Se (Table 3). The difference in the stability order of alumatranes and gallatranes can be traced to the strengths of individual M···N

(17) Leopold, K. R.; Canagaratna, M.; Philips, J. A. *Acc. Chem. Res.* **1997**, *30*, 57–64.

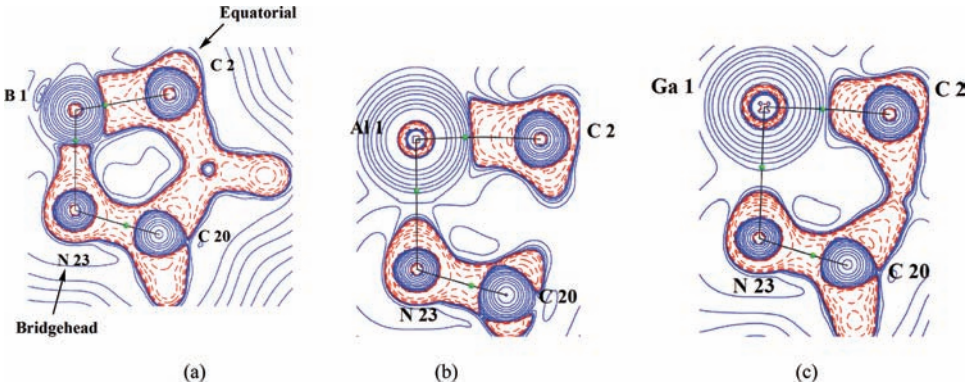

Figure 5. Contour plots of laplacian, $\nabla^2\rho$ (bcp), in a N···M−E plane of (a) carbaboratrane (M = B, E = CH_2), (b) carbaalumatrane (M = Al, E = CH_2) and (c) carbagallatrane (M = Ga, E = CH_2). Regions of charge depletion ($\nabla^2\rho > 0$) are denoted by solid blue lines while regions of charge concentration ($\nabla^2\rho < 0$) are denoted by dashed red lines. Green spheres denote bond critical points (BCPs), and the black solid line denotes bond paths.

and M−E bonds. While the Al···N bond lengths of oxa and thiaalumatranes are comparable ($\Delta r_{Al\cdots N}$ = 0.03 Å), the bond orders of Al−S bonds are much higher than that of Al−O bonds. Thus, thiaalumatrane is more stable than the oxa one. On the other hand, the Ga···N distances of oxa and thiagallatranes differ significantly ($\Delta r_{Ga\cdots N}$ = 0.09 Å). Due to the presence of a considerably shorter and, hence, stronger Ga···N bond, the stability of oxagallatrane is more than that of thiagallatrane even though the bond orders of Ga−S bonds are higher than that of Ga−O bonds.

3.3. Topological Analysis. The topology of electron density in a molecule can be analyzed using Bader's atoms in molecules theory (AIM).[9] Generally, for covalent interactions (also referred to as "open-shell" or "sharing" interactions), the electron density at the bond critical point (BCP), ρ_b, is large (> 0.2 a.u) while its laplacian $\nabla^2\rho$ is large and negative. On the other hand, for closed-shell interactions (e.g., ionic, van der Waals, or hydrogen bonds), ρ_b is small (< 0.10 a.u) and $\nabla^2\rho$ is positive. However, a clear distinction between the closed−shell and covalent type of interaction is impossible without determination of the local electronic energy density, $H(r)$. The local electronic energy density, $H(r)$, given by $H(r) = G(r) + V(r)$, where $G(r)$ and $V(r)$ are the local kinetic and potential energy densities, is negative for an interaction with significant covalent character and accounts for the lowering of potential energy of electrons at BCPs.[18] The magnitude of $H(r)$ reflects the "degree of covalency" present in a given interaction. Thus, some covalent (some polar bonds, donor−acceptor bonds, etc.) bonds are associated with positive values of $\nabla^2\rho$ and negative values of $H(r)$.

Table 4 contains the topological properties at the M···N bond critical point of group 13 atranes. All these group 13 atranes show a (3, −1) bond critical point at the M···N bond. The formation of (3, +1) ring critical points also supports the presence of the transannular interaction which indicates the formation of five-member rings in these molecules. As defined by Bader, the laplacian of electron density at BCP is given by $L(r) = \nabla^2\rho(r)$.[9] The accumulation of electron density, ρ_b, and a larger value of $L(r)$ along the bond path has an impact on the stability.[19a] Larger values of $L(r)$ and ρ_b result in local stabilization of the structure due to increased shielding of the nuclei of the bonded pair.[19b] All these group 13 atranes have considerable electron density at the transannular M···N bond critical point which increases with a decrease in transannular M···N distances (Figures 4, S1, and S2, Supporting Information). Hence, stronger bonds are associated with larger accumulation of ρ_b and a larger value of $L(r)$. The laplacians at the bond critical point, $\nabla^2\rho$, are all positive and increase with a decrease in transannular M···N bonds. This is in tune with previous theoretical studies.[20] It is evident from Table 4 that the electron density at the M···N bond critical point is highest for boratrane and lowest for alumatranes. Thus, the strength of transannular M···N interaction among group 13 atranes follows the order Al < Ga < B. This is also reflected in the computed WBI values (Table 2) of the respective bonds and delocalization index δ(M,N) (Table S2, Supporting Information). The laplacian, $\nabla^2\rho$, at the M···N bond critical points are all positive, and the local electronic energy densities are negative. Thus, the nature of transannular interaction in these group 13 atranes has significant covalent character which follows the order Al < Ga < B.

The contour plots of laplacian in the N···M−E plane for group 13 atranes are shown in Figure 5. It is evident from Figure 5 that the donation of the lone pair on the bridgehead nitrogen atom to the central group 13 atom is strongest in boratranes. This stronger donation in the case of boratranes is apparently caused by the favorable pyramidalization of the boron and the bridgehead nitrogen atom which draws them closer to each other. In contrast, geometrical constraints in heavier group 13 elements lead to weaker transannular interaction.

The calculated Ehrenfest force,[21] the only force acting on an atom in a molecule,[9] for the group 13 atom is attractive in every case, drawing them toward the bridgehead nitrogen atom. This attractive Ehrenfest force results in a stabilizing energy for the formation of the M|N_b (N_b is the bridgehead atom) surface. The external contribution to the nuclear−electron potential energy, at the metal center ΔV^ene(M), dominates over the own contribution

(18) Cremer, D.; Kraka, E. *Angew. Chem., Int. Ed. Engl.* **1984**, *23*, 627–628.

(19) (a) Gatti, C. *Z. Kristallogr.* **2005**, *220*, 399–457. (b) Gibbs, G. V.; Downs, R. T.; Cox, D. F.; Ross, N. L.; Boisen, M. B., Jr.; Rosso, K. M. *J. Phys. Chem. A* **2008**, *112*, 3693–3699.

(20) (a) Love, I. *J. Phys. Chem. A* **2009**, *113*, 2640–2646. (b) Boily, J. *J. Phys. Chem. A* **2003**, *107*, 4276–4285. (c) Henn, J.; Ilge, D.; Leusser, D.; Stalke, D.; Engels, B. *J. Phys. Chem. A* **2004**, *108*, 9442–9452.

(21) Ehrenfest, P. *Z. Phys.* **1927**, *45*, 455.

ΔV^0ne(M), which accounts for the stability of these molecules (Table S2, Supporting Information).

4. Conclusion

The nature of intramolecular M···N interaction, a key structural feature of group 13 atranes, is found to depend on the substituents at the equatorial position. The extent of this transannular interaction for lighter (M = B) group 13 atranes is also found to be a function of the degree of pyramidalization at the M and bridgehead nitrogen atom. However, the extent of transannular interaction for heavier (M = Al, Ga) group 13 elements is not consistent with the pyramidalization at the group 13 and bridgehead nitrogen atom. Heavier group 13 elements undergo very low pyramidalization, owing to their bigger size, and as a result, the transannular interaction becomes weaker. Also, the extent of transannular interaction in heavier group 13 elements is found to depend on the size of the equatorial groups. Bigger equatorial groups like Si, S, Se, etc. lead to deformation of the atrane cage to release the steric crowding and, hence, weaken the transannular interaction. Calculated stabilization energies of all the group 13 atranes are found to depend largely on the extent of transannular interaction with significant contribution coming in from M−E bond strengths. QTAIM analysis of the M···N bonds reveals that these bonds are characterized by: (i) low to moderate values of electron density, ρ_b (ii) positive values of the laplacian, $\nabla^2\rho$, and (iii) negative values of local energy densities, $H(r)$. Thus, on the basis of the negative values of local energy density, $H(r)$, it can be concluded that the M···N bonds of these molecules have significant covalent character which follows the order Al < Ga < B.[19] Ehrenfest forces for the group 13 atom are all attractive in nature, and the atomic contribution for the stability of these molecules comes from large negative values of external contribution to nuclear−electron potential energy at the group 13 center, ΔV^ene. We feel that our study will help the experimentalists in understanding the structural diversity of these classes of compounds and further help in realizing new and efficient atrane based catalytic systems as they are important reagents in various transformations.[10]

Acknowledgment. A.K.P. thanks the Department of Science and Technology (DST), New Delhi, for providing financial assistance in the form of a project (Project No. DST/FTP/CS-85/2005). A.K.G. thanks Tezpur University for an institutional fellowship.

Supporting Information Available: Tables S1 and S2, Figures S1 and S2, complete reference for Gaussian 03 (ref 15), and the Cartesian coordinates of the optimized geometries of all the group 13 atranes. This material is available free of charge via the Internet at http://pubs.acs.org.